

# Third Stage Laser for Three-Photon Absorption in Room Temperature Rubidium

**Marzouk M., Youssef**

Department of Physics, Middlebury College, Middlebury, VT

Project report for PHYS 0704

Sunday 22<sup>nd</sup> May, 2022

We present a scheme for three-photon excitation in room temperature rubidium. Using diode lasers we created an overlapping optical arrangement to follow the  $5S_{1/2} \rightarrow 5P_{3/2}$  (780-nm laser wavelength),  $5P_{3/2} \rightarrow 5D_{5/2}$  (776 nm), and  $5D_{5/2} \rightarrow 6P_{3/2}$  (1256 nm) cascade in room temperature  $^{85}\text{Rb}$  atoms, with principal quantum number  $n = 63$ . This is building on previous work done by Professor A. Goodsell at Middlebury College who has successfully created two-photon excitation in launched cold atoms [1]. We have created, and tested, parts of a proposed scheme that is both robust and affordable for creating Rydberg rubidium atoms. This setup is ideal for carrying out a range of quantum physics experiments and has been designed with integration into the already existing lab at Middlebury College in mind.

# **I Introduction**

Rydberg atoms, atoms in states of high principal quantum number  $n$ , are atoms with exaggerated properties. This results in them being more susceptible to influences from external magnetic and electric fields, making them great candidates for study of quantum mechanical properties of atoms. While they have been studied intensely since the 1970s, they have played a role in atomic physics since the beginning of quantitative atomic spectroscopy. The original method of studying Rydberg atoms was by absorption spectroscopy, and it remains a generally useful technique [2]. Variants of detection were developed that included dye lasers to populate an excited state preferentially, allowing the absorption spectrum of the atoms in the excited state to be recorded. However, most of modern work is done by detecting the excited Rydberg atoms themselves rather than their absorption spectra.

Rydberg atom detection can be accomplished in two ways. First, after being optically excited, their slow decay to lower states radiates visible fluorescence. Second, we can detect the Rydberg atoms by ionizing them via collisional or field ionization. This can be done easily due to the outermost electron being in a large weakly bounded orbit. We aim to create a model for the former mode of detection at this time for observations of atoms at room temperature. This sets the stage for direct detection of cold Rydberg atoms later. Following the work previously done at Middlebury College, we designed a model for Rydberg rubidium-85. This element is relatively easy to convert to a vapor and has an emission and absorption spectrum that allows for the use of cheaper infrared diode lasers for excitation. The following is a discussion and summary of two major elements in the model: The third-stage laser tuning and optimization and the experimental setup for detecting absorption.

## **II Third stage characterization**

In a paper published in 2009, Thoumany, et al. created a scheme for observing three-photon absorption in a room temperature rubidium gas cell. We modeled our excitation scheme after their work and, as a result, opted for following a similar three-laser cascade outlined in Fig. 1. Previous work in Professor Goodsell's lab has succeeded in measuring excitation with the first and second stage lasers, therefore, this work has been primarily focused on proper implementation of the third stage (1256 nm) of the excitation scheme.

### **II. (i) Power and Intensity**

As part of the characterization of the laser, we recreated performance plots from the specification sheet to better understand the performance of the laser. Previous work by Thoumany, et al. has found success in using the third stage laser at 5 mW and we aim to compare our laser's performance to that standard. We measured the laser's power output across the whole tuning range while the laser's drive current,

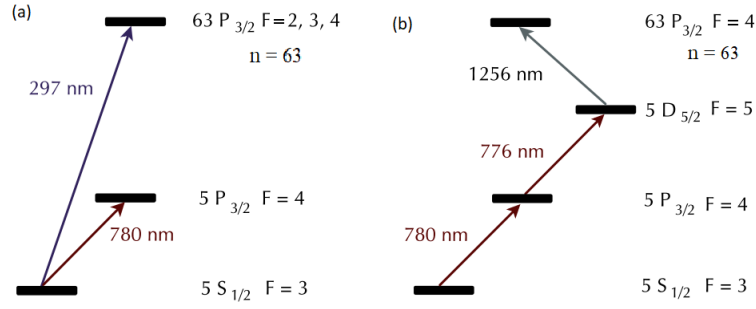


Fig. 1. Two level schemes for Rydberg rubidium atoms. In (a) the Rydberg atoms are excited in one step using a 297-nm laser. The 780-nm laser is used to confirm absorption. In (b) the Rydberg atoms are excited using three infrared lasers (Excitation scheme image sourced from Thoumany, et al. 2009 [3]).

$I_{LD}$ , is set to 300 mA mimicing a plot from the spec sheet. From these results (Fig. 2) we found that our measured power was 0.16 mW—a factor of 10 lower than expected based on the specification [4]. When compared to Thoumany, et al. our third stage was a factor of 50 lower power than their laser. This is a potential cause for concern as our lower power may not be enough for base saturation in the third excitation stage. The first stage power was never specified in previous literature, however, data was collected after running the second stage at intensities above base saturation and consequences of this were asymmetries in absorption data, leading Thoumay, et al. to run their 780 nm laser below saturation intensity. The second stage was recorded to be running at 2 mW which we can replicate using the current lab at Middlebury College [3].

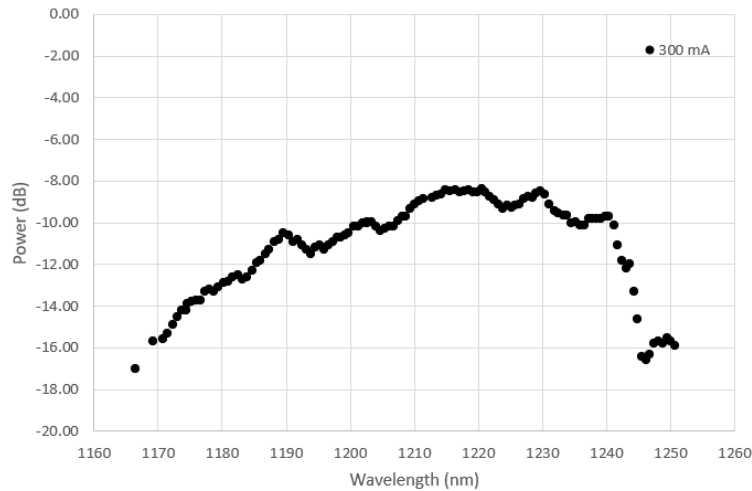


Fig. 2. Measured power output of the laser while scanning the full tuning range with a running current  $I_{LD} = 300$  mA and temperature control at  $21^{\circ}\text{C}$ .

We measured a peak power of 0.16 mW at the laser's typical operating wavelength of 1220 nm.

In light of the shortcomings of the power output, we opted to measure the beam size to get a

better understanding to the intensity of the light. We decided on an experiment that places a razor blade approximately where we would expect all three lasers to intersect inside the rubidium cell. We then measure the power while scanning the razor's edge in front of the laser beam. We expect to see a plot that decreases as more beam light is blocked from reaching the photodetector by the razor. Figure 3 displays the results of this experiment scanning only the beam width after 35-36 inches of beam travel after exiting the laser cavity. We measured beam cross section to be a measurement from 10% of the measured intensity to 90%. Assuming a purely circular beam intersection we can estimate the intensity to be 25 - 35 mW/cm<sup>2</sup>. However, from qualitative observation we believe that the laser beam is vertically larger than it is wide, consequently, the previously stated intensities are in all likelihood over estimates to the true intensity. Beam vertical size was never explicitly measured.

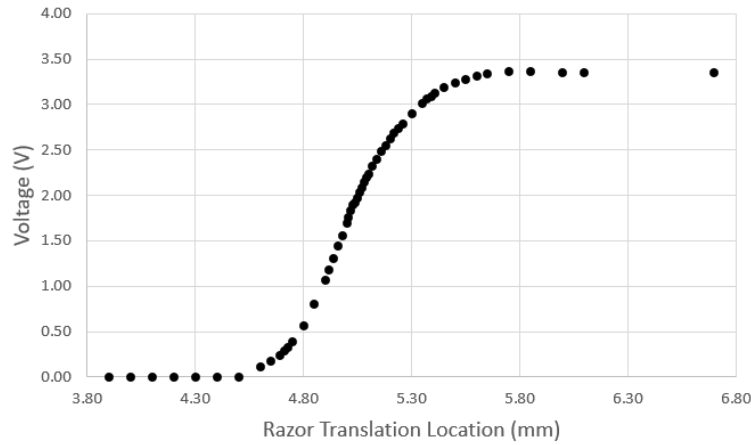


Fig. 3. Beam width results after scanning a razor blade's edge in front of the beam after  $\approx 3$ ft. of beam travel. Measurements taken with laser wavelength set to 1256 nm.

Voltage is the raw output of the photodetector.

## II. (ii) Wavelength

Our chosen laser is a diode laser in a Littrow configuration. This configuration allows us to take a laser light—spanning a small range of wavelengths—and scatter it using a grating. This grating allows us to have different wavelengths of light correspond to different locations in space. By adjusting the angle of this grating we can direct whichever wavelength we would like to use into the gain chip to amplify our desired running wavelength. The details of this diffraction set up and relative beam paths can be seen in Fig. 4.

This approach aims to excite single hyperfine states in rubidium. As these states are separated by just a few kHz, laser frequency tuning and precision was of the utmost importance. Following the Thoumany paper we want to create a laser with the ability to modulate the frequency by 5 MHz ( $\sim 0.00003$  nm) increments. Our approach to tuning the laser wavelength is organized as a two-step process. First, we completed a full characterization of the laser at different operating currents

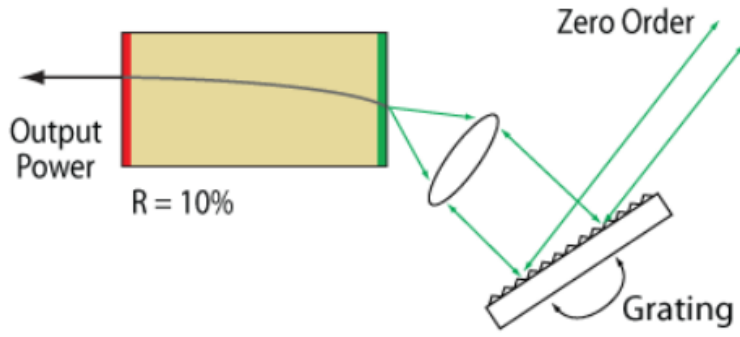


Fig. 4. This is a schematic of the laser pathway incident on the grating and scattering onto the collimating lens in the Littrow configuration from the Thorlabs tunable laser kits guide [5].

and temperatures. This mapped the range of wavelengths we can achieve and the stability of both the output wavelength and temperature controller. From this characterization we decided on running conditions that would allow us to reach 1256 nm and have adjustability without sacrificing temperature stability. These results are summarized in Fig. 5.

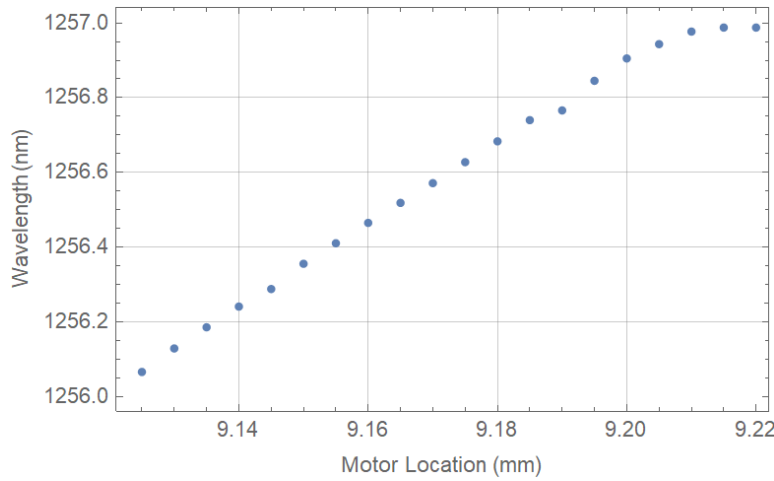


Fig. 5. This is the culmination of the full laser wavelength characterization with these running parameters:  $I_{LD} = 100.00(5)$  mA,  $T_{SET} = 11.420(10)$  k $\Omega$ . These operating conditions allow us to span 1256-1257 nm with <4 GHz increments via grating angle alone (not explicitly shown in figure). Note that the "angle" of the laser is specified as a distance. This distance is determined by a translationally linear motor location that adjusts the angle of the grating that is never explicitly measured.

We also worked towards more accurately determining the absorption wavelength of the third stage, however, the laser frequency range of absorption is small and as a result we attempt to create a scheme for stable detuning of the laser frequency of approximately 5 MHz, again, following in the footsteps of Thoumany et al. Detuning involves slightly altering the laser wavelength from being "tuned" to the correct wavelength where we observe absorption. These small adjustments in wave-

length can allow us to create smoother absorption plots to confirm Rydberg excitation. This plot will let us clearly see absorption when tuned and as we detune the laser this absorption begins to fade. From Ref. [3] we see that absorption spans 100 MHz ( $\sim 0.0006$  nm). This is much higher precision than grating angle adjustments will allow. We opted to modulate the running current,  $I_{LD}$ , of the laser to attempt this finer control.

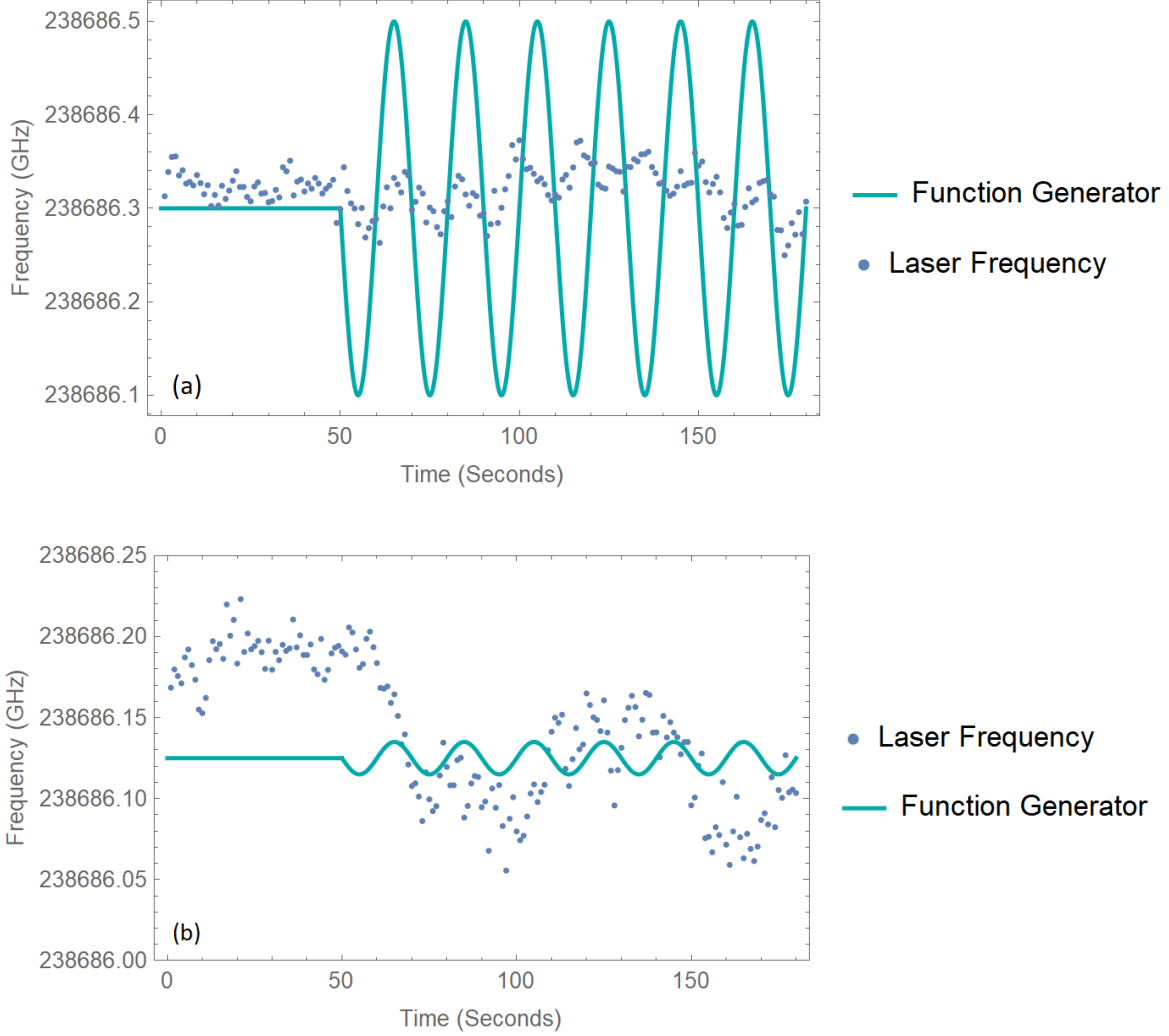


Fig. 6. These plots summarize efforts in detuning the laser frequency by increments of 5 MHz through current modulation. Blue points indicate recorded frequency and the function generator is the input of the current,  $I_{MOD}$ , which allows us to change laser running current,  $I_{LD}$ , in smaller increments. The function generator amplitudes are not to scale, but only indicate amplitudes relative to each other across (a) and (b). (a) has an input sine function of 20 mV amplitude corresponding to a  $\pm 1$ -mA modulation. (b) has an input sine function with 1 mV amplitude corresponding to  $\pm 0.05$ -mA modulation in  $I_{LD}$ .

Without modulation we observed that the laser will often fluctuate 70 MHz in frequency. Figure 6(a) is a proof-of-concept experiment. The programmed modulation was greater than the laser's

ambient wavelength fluctuation to more easily confirm our expected behavior. As predicted, smaller wavelength modulation was more difficult to observe. Figure 6(b) shows promise in general trends. The frequency seems to be fluctuating, however, the noise from the ambient laser fluctuations makes it so we cannot qualitatively confirm detuning on the scale of 5 MHz.

## II. (iii) Polarization

Knowledge of the initial polarization of the third stage laser would better inform our optical layout. Polarization is a property of the third stage laser that has not been determined and finalized from previous literature. This gives us the freedom to experiment with various polarizations for optimal absorption results. However, manipulation of the laser polarization requires characterization and knowledge of polarization upon exiting the laser cavity. To characterize the polarization, we used a polarizing beam splitter (PBS) in combination with a half-wave plate to determine both configuration (linear/elliptical) and orientation of the laser polarization. Table I outlines the results of our observations. We found that given a half waveplate in series with the PBS, we observed >90% reflectance and >86% transmission of the laser light, which is consistent with expected total transmission and reflection data from the PBS specification sheet. This data informs our conclusion of the laser light polarization is linear before manipulation.

Table I. Results of measured voltage output after the polarizing beam splitter (PBS). Fraction values compare measured values to voltage measurements taken before the half-waveplate and PBS.

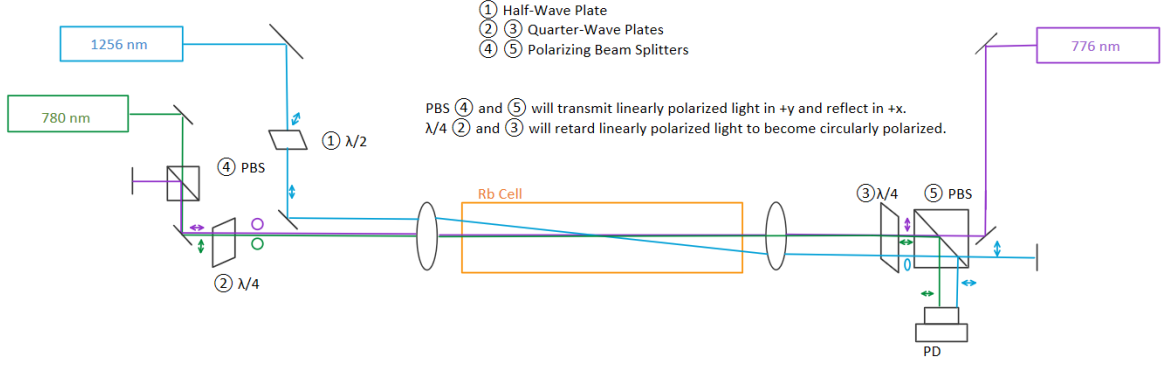
	Voltage (V) $\pm$ 13 mV	Power (mW) $\pm$ 2%	Fraction of total light <sup>a</sup>
Reflected Min.	0.14	0.011	0.08
Reflected Max.	1.59	0.12	0.91
Transmitted Min.	0.14	0.004	0.03
Transmitted Max.	0.14	0.115	0.87

<sup>a</sup>. Fraction values are with respect to measured voltage before PBS and half wave plate.

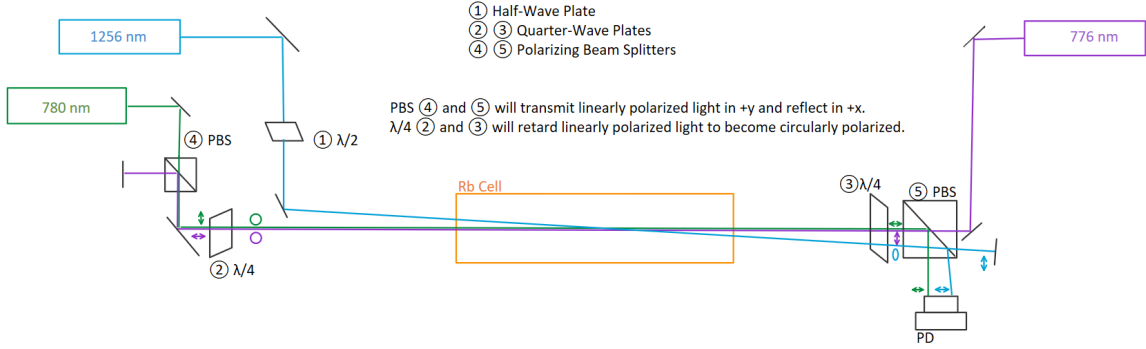
## III Description of the optical layout

Both first and second stage lasers have their independent stabilization circuits and are resonant with the  $5S_{1/2} \rightarrow 5P_{3/2}$  and  $5P_{3/2} \rightarrow 5D_{5/2}$  transitions, respectively [1]. The third stage laser is a grating stabilized diode laser (Fig. 4) and is resonant with the final  $5D_{5/2} \rightarrow 6P_{3/2}$  transition. Our optical scheme—seen in Fig. 7—aims to take the first and second stage lasers, and circularly polarize them to increase the probability of absorption. These two stages are sent counter propagating through the warm rubidium cell and intersect at a point by means of a convex lens (Fig. 7a) or mirror (Fig. 7b) [6].

The final laser is then linearly polarized and sent copropagating with the first stage. The angle of the linear polarization of the final stage is fully adjustable and will be optimized, if possible, for absorption.



(a)



(b)

Fig. 7. Two proposed beam paths with different methods of combining all three lasers to intersect at a point in the rubidium cell. (a) Laser lights crossing is accomplished by two convex lenses on either side of the cell. (b) An angled mirror is used to cross the third stage with the first two. Arrows, circles and ovals indicate polarization direction of either linear, circular or elliptical respectively.

## IV Conclusion

In summary, we have created a prototype for three-photon absorption for warm rubidium. However, some of the larger holes in our work that need further research are the power of the third stage laser and further analysis of the laser's intensity. The power output being so much lower than what we expect from specification is quite alarming. Even more so when none of the previous literature has claimed success with three photon absorption with less than 3 mW of power. The 1256-nm laser's intensity could also see further analysis. A measurement of the vertical extent of the beam cross section and creation of a Gaussian fit of the laser intensity are both areas that are ready to be measured and analyzed. Following this work, future research is well equipped to align all three lasers into a warm rubidium cell and look for absorption. Success in warm rubidium absorption would promote implementation of the third stage laser into the cold rubidium setup at Middlebury College for further



research in quantum physics experiments.

## **V Acknowledgements**

I am extremely grateful to professor A. Goodsell at Middlebury College for allowing us to use both space and equipment in her lab to conduct the experiment. She was also a great resource, and guiding hand, throughout providing both vital experience and advice. I would also like to thank the SRPS at Middlebury College and A. Goodsell for helping fund the research.

## Bibliography

- [1] R. Gonzalez, E. Alejandro, E. Erwin, and A. L. Goodsell, “Two-photon excitation of launched cold atoms in flight,” *Journal of the Optical Society of America B*, vol. 34, no. 6, p. 1090, Jun. 2017. [Online]. Available: <https://opg.optica.org/abstract.cfm?URI=josab-34-6-1090>
- [2] T. F. Gallagher, *Rydberg Atoms*, ser. Cambridge Monographs on Atomic, Molecular and Chemical Physics. Cambridge University Press, 1994.
- [3] P. Thoumany, T. Germann, T. Hänsch, G. Stania, L. Urbonas, and T. Becker, “Spectroscopy of rubidium Rydberg states with three diode lasers,” *Journal of Modern Optics*, vol. 56, no. 18-19, pp. 2055–2060, Oct. 2009. [Online]. Available: <http://www.tandfonline.com/doi/abs/10.1080/09500340903180525>
- [4] Thorlabs, “Thorlabs - SAF1175S Mounted SAF Gain Chip, Half Butterfly Pkg, CWL = 1220 nm, SM Fiber.” [Online]. Available: <https://www.thorlabs.com/thorproduct.cfm?partnumber=SAF1175S>
- [5] “Tunable Lasers: Prealigned Littrow and Littman Kits,” Dec. 2017. [Online]. Available: <https://www.thorlabs.com/catalogpages/Obsolete/2017/TLK-L1550R.pdf>
- [6] L. A. M. Johnson, H. O. Majeed, and B. T. H. Varcoe, “A three-step laser stabilization scheme for excitation to Rydberg levels in 85Rb,” *Applied Physics B*, vol. 106, no. 2, pp. 257–260, Feb. 2012. [Online]. Available: <http://link.springer.com/10.1007/s00340-011-4805-8>